

Elucidating the Drug Release from Metal–Organic Framework Nanocomposites via In Situ Synchrotron Microspectroscopy and Theoretical Modeling

Barbara E. Souza, Lorenzo Donà, Kirill Titov, Paolo Bruzzese, Zhixin Zeng, Yang Zhang, Arun S. Babal, Annika F. Möslein, Mark D. Frogley, Magda Wolna, Gianfelice Cinque, Bartolomeo Civalleri,* and Jin-Chong Tan*

Cite This: *ACS Appl. Mater. Interfaces* 2020, 12, 5147–5156

Read Online

ACCESS |

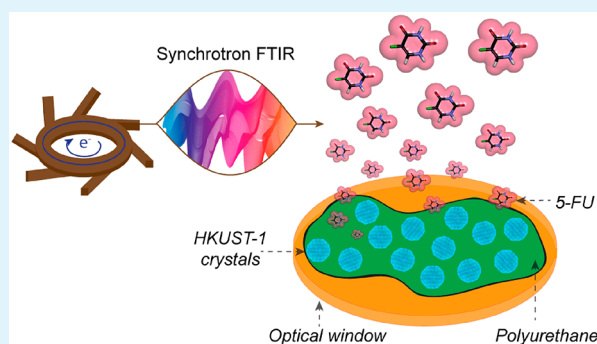
Metrics & More

Article Recommendations

Supporting Information

ABSTRACT: Nanocomposites comprising metal–organic frameworks (MOFs) embedded in a polymeric matrix are promising carriers for drug delivery applications. While understanding the chemical and physical transformations of MOFs during the release of confined drug molecules is challenging, this is central to devising better ways for controlled release of therapeutic agents. Herein, we demonstrate the efficacy of synchrotron microspectroscopy to track the in situ release of 5-fluorouracil (5-FU) anticancer drug molecules from a drug@MOF/polymer composite (5-FU@HKUST-1/polyurethane). Using experimental time-resolved infrared spectra jointly with newly developed density functional theory calculations, we reveal the detailed dynamics of vibrational motions underpinning the dissociation of 5-FU bound to the framework of HKUST-1 upon water exposure. We discover that HKUST-1 creates hydrophilic channels within the hydrophobic polyurethane matrix hence helping to tune drug release rate. The synergy between a hydrophilic MOF with a hydrophobic polymer can be harnessed to engineer a tunable nanocomposite that alleviates the unwanted burst effect commonly encountered in drug delivery.

KEYWORDS: nanocomposite, drug delivery, 5-fluorouracil (5-FU), metal–organic framework (MOF), drug@MOF, in situ microspectroscopy, synchrotron radiation, density functional theory (DFT)



INTRODUCTION

The concept of employing metal–organic frameworks (MOFs) as a porous vessel to host drugs as a guest molecule, that is, “drug@MOF” systems, holds promise as a pharmaceutically efficient carrier to achieve sustained release of various therapeutic molecules.^{1–3} Although progress has been made in the recent years,^{4,5} the prolonged, well-controlled, targeted delivery of therapeutic agents remains a challenge in the field. For example, research on the delivery of anticancer drugs currently seeks to improve the traditional direct administration routes to mitigate any undesirable side effects and poor biodistribution.^{6–8}

More recently, strategies combining porous materials and organic polymers to yield a bespoke composite present an alternative way forward to avoid the rapid and uncontrolled release of the encapsulated drug molecule, the so-called “burst effect”.⁹ We have recently reported the application of a mechanochemical method to accomplish the in situ encapsulation of the anticancer drug 5-fluorouracil (5-FU), confined within the HKUST-1 framework [Cu₃(BTC)₂; BTC = benzene-1,3,5-tricarboxylate], resulting in the 5-FU@HKUST-1 sys-

tem.¹⁰ However, HKUST-1 is a water-sensitive MOF, which degrades rapidly in the presence of humidity.^{11,12} In this study, we demonstrate that 5-FU@HKUST-1 can be easily combined with a biocompatible polymer like polyurethane (PU) to fabricate the 5-FU@HKUST-1/PU composites that could suppress the burst effect.^{13–15} The presence of a polymeric matrix can significantly enhance the aqueous stability of certain MOFs that have a huge potential for hosting a plethora of drug molecules, but suffer from poor water stability.¹⁶ Specifically, HKUST-1 has been selected not only due to its poor water stability, but also due to the presence of coordinatively unsaturated metal sites (CUS) that could act as strong binding sites for attaching different polar guest molecules.¹⁰ The combination of polymer and MOFs represents an effective way of providing a suitable scaffolding to the MOF while

Received: November 28, 2019

Accepted: January 6, 2020

Published: January 6, 2020

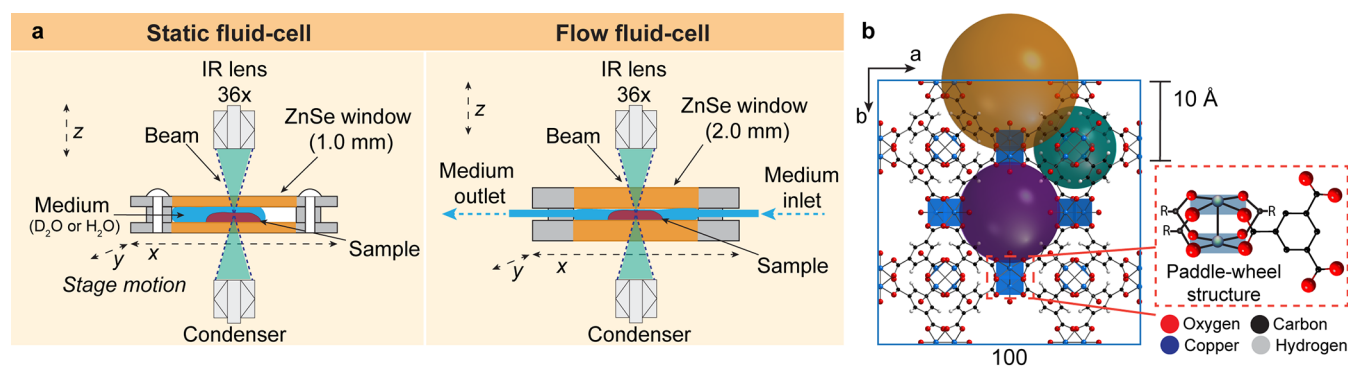


Figure 1. Experimental setup for SR-microFTIR spectroscopy measurements and representation of the drug@MOF samples under study. (a) Schematic of the static- and flow-fluid cells and sample arrangement (not to scale). (b) Crystal structure of HKUST-1 highlighting the three different types of pores in the structure with diameters of 5 (green), 11 (purple), and 13.5 Å (yellow), and an illustration of the paddle-wheel moiety.

harnessing its great potential as a drug delivery system (i.e., the presence of unsaturated Lewis metal sites acting as strong binding site, thus creating a tunable drug@MOF/polymer platform for therapeutic applications, such as the topical treatment of skin conditions via the fabrication of functional wound dressing devices.^{17,18}

Understanding the release of (guest) drug molecules from host frameworks is, generally, carried out using *ex situ* techniques (e.g., sample and separate, continuous flow, dialysis membranes)¹⁹ that are more appropriate for establishing the drug release kinetics. However, to gain a deeper comprehension of the drug release process itself, one should observe both the chemical and physical changes in the drug-loaded samples *in situ*. Continuous monitoring of such changes is, however, difficult, as these can occur in an accelerated manner and hence not easily probed by the conventional techniques.

Analytical studies to construct drug release profiles of drug@MOF systems rely on a stepwise approach, where aliquots are periodically collected from the released media and the drug concentration is determined via UV-vis spectroscopy and liquid chromatography.^{20–22} Although the stepwise measurements yield drug release profiles, they do not reveal the underlying chemical and physical mechanisms or structural transformation occurring during the guest release process. These dynamical changes are key to correlating the guest–host interactions of drug@MOF systems.

To address these limitations, herein, we present an *in situ* strategy to probe the release of 5-FU from HKUST-1/PU membrane composites. We use synchrotron radiation Fourier transform infrared microspectroscopy (SR-microFTIR) in Beamline B22 MIRIAM at the Diamond Light Source,^{23,24} which allows broadband measurements to be conducted with a high signal-to-noise ratio. We follow the transformations of the host framework through the evolution of vibrational bands that are specific to the guest and the host structures, further substantiated by *ab initio* density functional theory (DFT) calculations for additional insights into drug–MOF interactions and their energetics.

RESULTS AND DISCUSSION

We performed SR-microFTIR spectroscopy experiments in two different fluid-cell setups (i.e., static and flow liquid cells) to study the molecular structural changes of the guest–host assembly of 5-FU@HKUST-1/PU composite and its constituents during the release of drug molecules. We will begin by considering the results of the static experiments performed

under deuterated water (D₂O) exposure. Utilizing DFT theoretical calculations, we then shed light on the energetics of drug–MOF interactions responsible for the adsorption and release of the encapsulated drug molecules. Finally, we examine results from the flow experiments subject to a combination of D₂O/H₂O, revealing the synergy of the polymer matrix and MOF combination that enables the composites to suppress the unwanted burst effect.

Static-Cell Measurements. Figure 1a shows a schematic representation of the experimental setups used in this study (see Figure S1 in the Supporting Information (SI) for additional details of the experimental setup). Static fluid-cell experiments were performed using samples listed in Table S1, individually inserted into a customized liquid cell between two zinc selenide (ZnSe) circular windows separated by a 10- μ m thick Teflon spacer. Two microliters of the chosen medium (D₂O) were pipetted onto the sample, and the cell was sealed (see experimental protocols in the Methods section). To select specific sites within the samples, images were collected under visible light via the IR microscope (Figure S2). For the infrared measurements in different media, the frequency of a molecular vibration depends on the masses of the vibrating atoms. Therefore, absorption bands of D₂O appear at lower wavenumbers than in H₂O (Figures S3 and S4). In the ranges of 1500–1750 cm⁻¹ (H–O–H bending) and 1150–1300 cm⁻¹ (D–O–D bending), H₂O or D₂O modes, respectively, overlap with important vibrational bands of the drug molecule present in the 5-FU@HKUST-1 samples. Therefore, the monitoring of the 5-FU drug release was carried out with a complementary set of experiments performed in H₂O and D₂O, respectively, to fully capture the evolution of drug peaks in the spectral range of interest (650–2000 cm⁻¹). Importantly, the release of the drug molecules can be tracked by the progressively decreasing intensity of the 5-FU peaks identified in the 5-FU@HKUST-1 samples.

Detailed characterization of the composite samples was performed and described in the SI. The samples were characterized via thermogravimetric analysis (Figures S5 and S6), where the level of drug encapsulation within HKUST-1 was determined to be ~14.0 wt %. Comparison of drug loading with various other 5-FU@MOF systems is presented in Table S2. The characterization of the morphology of the HKUST-1 crystals and 5-FU@HKUST-1/PU membranes (Figures S7 and S8, respectively) was performed via scanning electron microscopy (SEM) and atomic force microscopy (AFM).

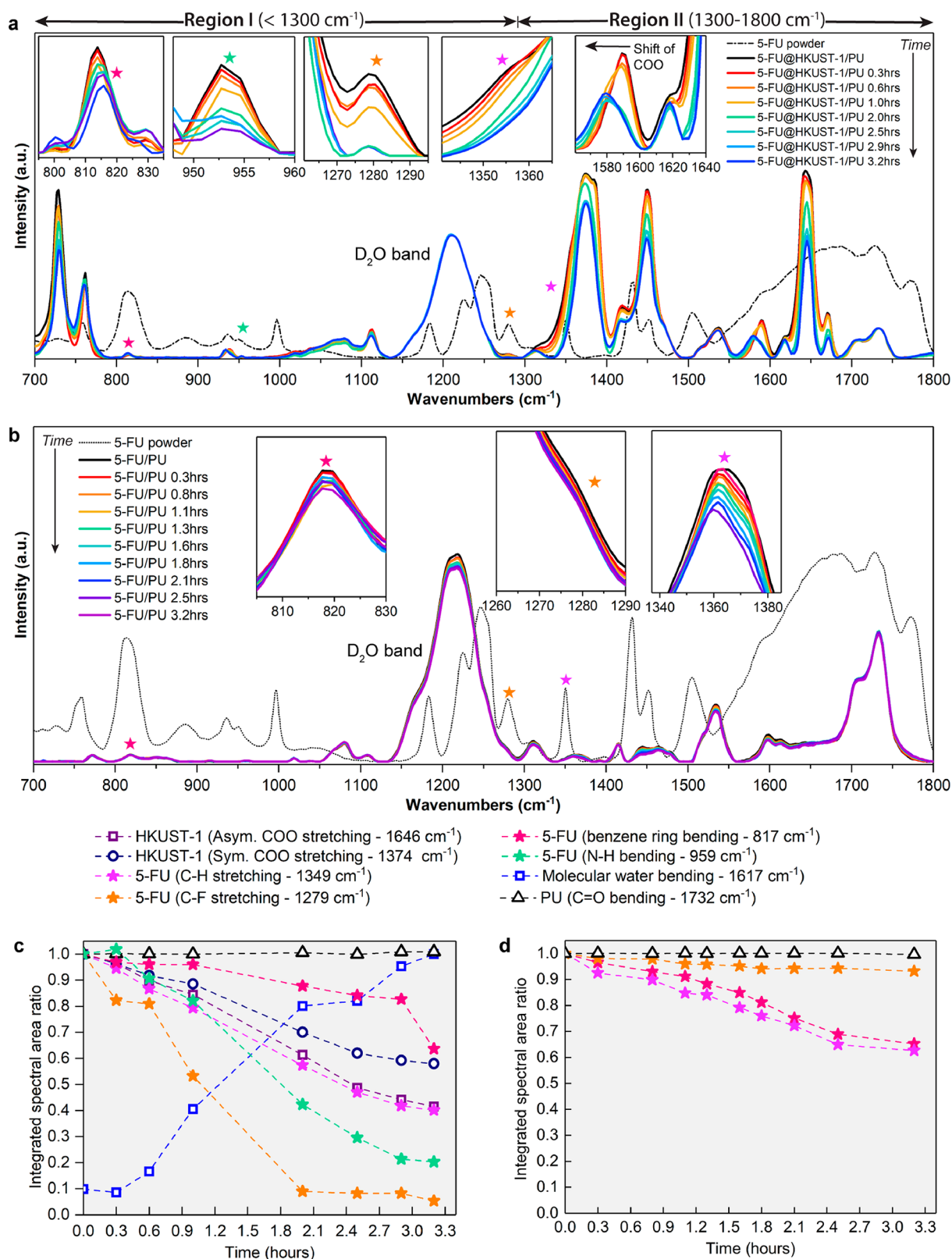


Figure 2. SR-microFTIR spectra obtained by static fluid-cell measurements. Evolution of (a) 5-FU@HKUST-1/PU and (b) 5-FU/PU membranes, collected over a period of 3.2 h. Insets show in detail the changes observed to drug molecule related peaks and important HKUST-1 peaks. 5-FU powder spectrum was scaled down by a factor of 0.7 to facilitate the comparison with the composite spectra. In panel b, the spectra of a few time series were omitted for clarity, causing a small mismatch between the time intervals presented in panels a and b. However, the overall time analyzed had remained the same. Integrated spectral area ratios of selected peaks of (c) 5-FU@HKUST-1/PU and (d) 5-FU/PU, demonstrating the evolution of vibrational modes intensity in HKUST-1 framework, 5-FU drug, and molecular water. The PU peak at 1732 cm^{-1} (C=O bending) was chosen as a reference because of the absence of any changes with time recorded for this band.

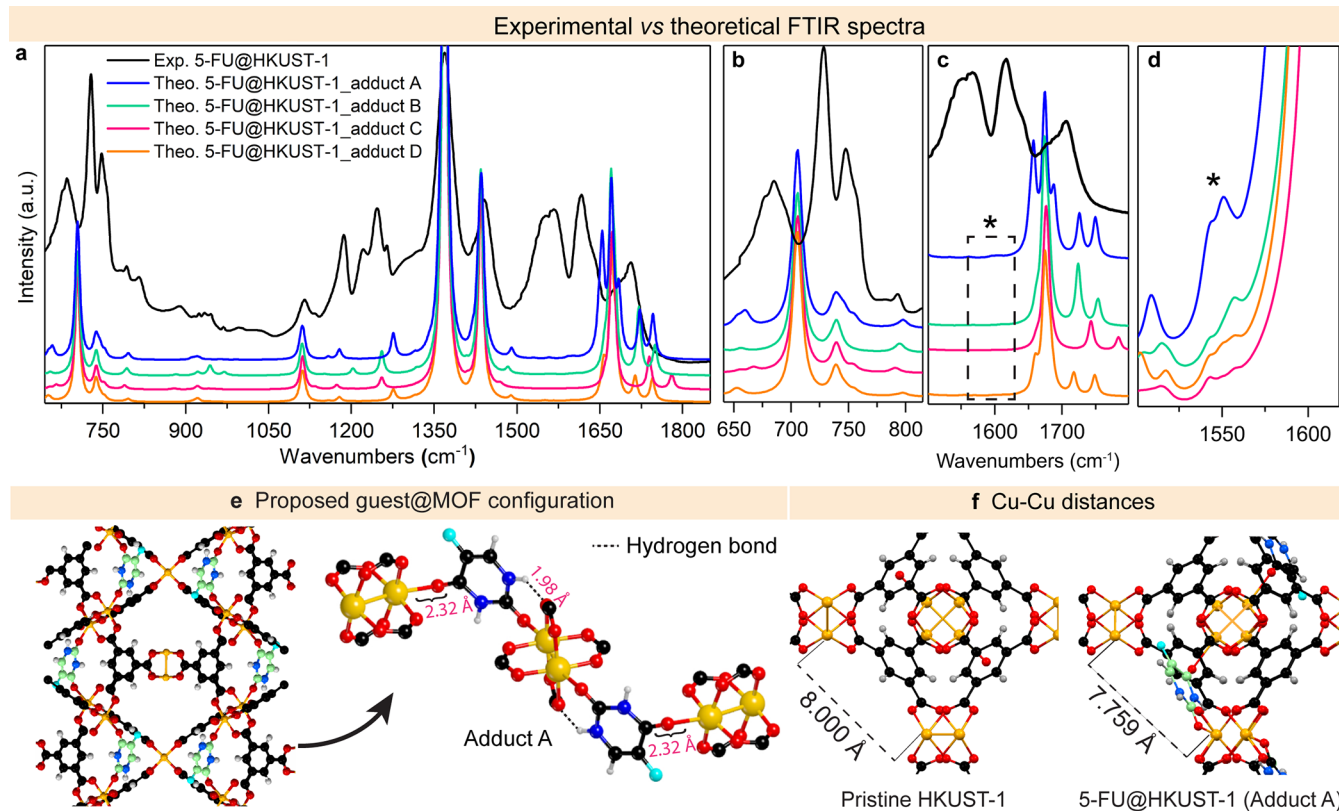


Figure 3. Results from DFT calculations. (a) Comparison of experimental (ATR-FTIR) and calculated spectra of 5-FU@HKUST-1 for the four possible host–guest configurations, termed adducts A–D. Closer look at different spectral regions showcasing the better match between adduct A spectrum and the experimental data when contrasted with other configurations: (b) 650–810 cm^{-1} , (c) 1500–1750 cm^{-1} , and (d) zoom-in of the peak $\sim 1550 \text{ cm}^{-1}$, which shows the low intensity region (due to the adopted DFT basis set). Note that a scaling factor (i.e., 0.95) was applied to the DFT spectra in panels a–d to eliminate common shifts resulting from the ab initio calculations and to match the frequencies against the experimental spectrum. (e) Proposed guest–host interaction obtained from DFT. In the schematic, 5-FU interacts with two different paddle-wheel sites through oxygen atoms while establishing hydrogen bonds with the carboxylate groups. (f) DFT optimized structure showing the Cu–Cu distances between adjacent paddle-wheels in pristine HKUST-1 (left) and 5-FU@HKUST-1 (right). Color code: O in red, C in black, H in gray, Cu in yellow, N in navy blue, and F in turquoise. Carbon atoms in the drug molecules were displayed in green to show the position of the guest molecule.

Figure 2a and 2b contrasts the time-dependent evolution of FTIR spectra of the 5-FU@HKUST-1/PU and 5-FU/PU samples. Because of the high loading of MOF within polymer in the composites (85 wt % of HKUST-1), the spectra of 5-FU@HKUST-1/PU were mainly dominated by the intense vibrational bands of the HKUST-1 framework. However, it is possible to distinctly identify 5-FU modes associated with the ring bending (δ -ring at 817 cm^{-1}) and N-H bonds (954 cm^{-1}), stretching of C-F (1279 cm^{-1}), and C-H bonds (1349 cm^{-1}) of 5-FU, as confirmed through the analysis of powder spectra (Figure S9). Figure 2c and 2d shows the time evolution of the integrated spectral area of selected HKUST-1, 5-FU, molecular water (H_2O), and PU peaks of 5-FU@HKUST-1/PU and 5-FU/PU composites, respectively. PU peaks were used as a reference due to the inert nature of the polymer upon water exposure. The values presented at different time points were normalized against the initial area value (hereafter referred only as “area”). The HKUST-1 structure is composed of dimers of Cu^{2+} ions chelated by four benzene-1,3,5-tricarboxylate (BTC) bridges, forming a moiety known as the paddle-wheel (see Figure 1b). With respect to the vibrational modes of HKUST-1, the spectra of the composites can be divided into two regions. Region I ($<1300 \text{ cm}^{-1}$), shows bands assigned to the out-of-plane vibrations of benzene ring while region II ($1300\text{--}1800 \text{ cm}^{-1}$) is mainly associated with the vibrations of the carboxylate

groups. Both are parts of the BTC linker. Specifically, the bands at 1646 and 1590 cm^{-1} and at 1450 and 1374 cm^{-1} in region II correspond to the asymmetric and symmetric stretching of the carboxylate groups, respectively (see Figure S10). The three typical microporous sites in HKUST-1 structure (5 , 11 , and 13.5 \AA in diameter), possessing different hydrophilic characters, are schematically represented in Figure 1b. Water molecules can only penetrate the larger pores of the framework,^{25,26} where they start hydrolyzing the Cu-O bonds in the paddle-wheel and so breaking down the crystalline structure of HKUST-1.¹¹ To track the permeation of media through the polymer matrix, we track the bending mode of molecular water at 1617 cm^{-1} (see Figure S4). It is important to note the increasing presence of the H_2O band in the sample during measurements performed under D_2O exposure, despite the stability of the D_2O band ($\sim 1200 \text{ cm}^{-1}$) throughout the experiment (i.e., no significant bulk D–H exchange in the liquid was detected). This observation suggests that a small amount of D–H exchange occurs within the pores of HKUST-1, with the substitution of hydrogen atoms found on the framework. As such, this confirms the ingress of D_2O into the sample, showing an increasing penetration with longer exposure, trackable with the synchrotron microFTIR probe. The complete description of the vibrational modes of the composites, 5-FU, and PU are summarized in Table S3.

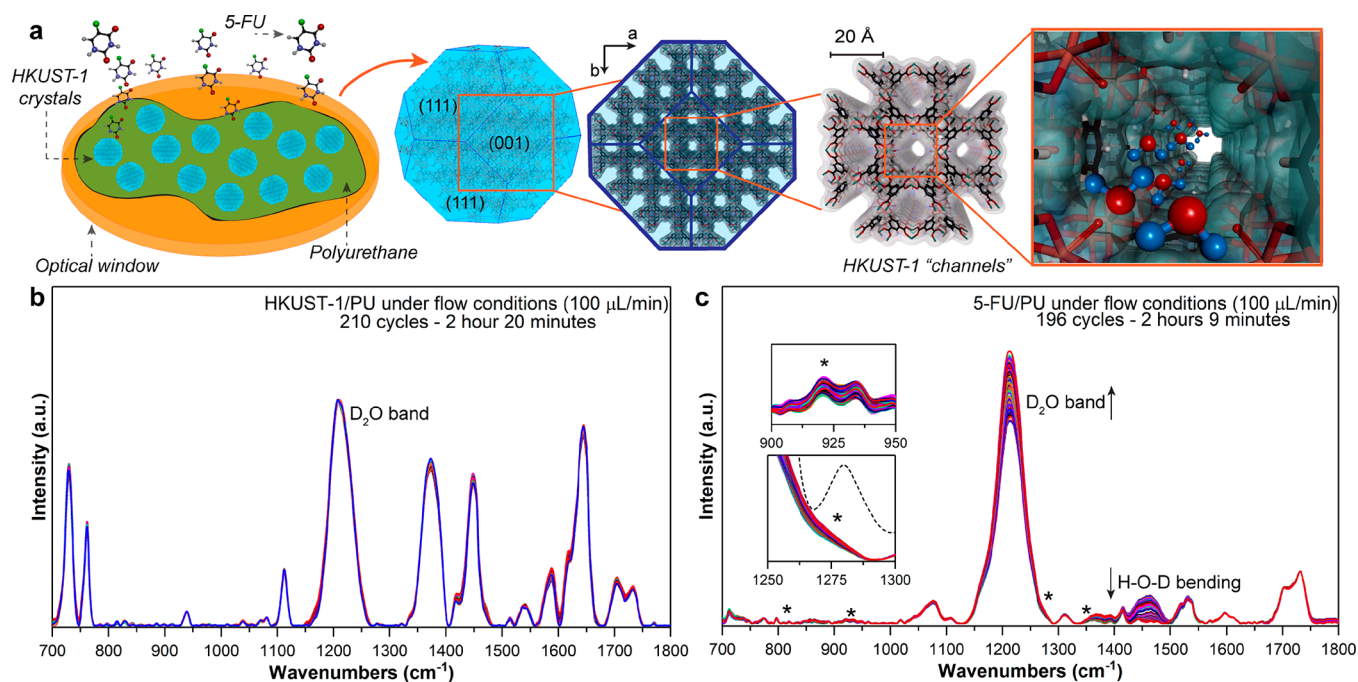


Figure 4. Flow-cell measurements of polymeric composites. (a) Schematic representation of HKUST-1 crystals and hydrophilic “channels” responsible for the permeation of water into the polymeric matrix and release of 5-FU molecules from the polymeric membrane. Time-resolved FTIR spectra collected during the flow experiments. (b) HKUST-1/PU membrane under D₂O flow shows absence of any change to MOF vibrational bands. (c) 5-FU/PU membrane spectra, showing the increase in intensity of D₂O band and decrease of H₂O which demonstrates the stabilization of D₂O flow. Asterisk marks the position of drug peaks in the composite spectra. Color code: O in red, C in black, H in gray, Cu in orange, N in purple, and F in green. Hydrogen atoms in the water molecules are shown in blue.

Within regions I and II, three important features must be highlighted. First, in Figure 2a, with time progression the observed decrease in intensity of the vibrational peaks and integrated spectral area values of drug and framework peaks. Second, the shift of the band detected at 1590 cm⁻¹ shown in the inset of Figure 2a, associated with the symmetric stretching of the carboxylate groups in HKUST-1. This shift can be assigned to modifications in the coordination of the carboxylate groups, indicating changes in chemical and physical interactions surrounding the HKUST-1 paddle-wheel environment. Last, in Figure 2c and d, the evident differences in the kinetics of the 5-FU drug molecules being released from the 5-FU/PU sample versus the 5-FU@HKUST-1/PU composite membrane.

Detailed analysis of the evolution of the FTIR spectra of 5-FU@HKUST-1/PU shows that within 1 h of continuous exposure to D₂O, the HKUST-1 framework was not greatly affected. After 2 h, the decrease of the framework vibrational bands intensity was observed. These changes are accompanied by the increase in intensity of the band at 1617 cm⁻¹, showcasing penetration of water molecules into the composite and their interaction with HKUST-1. The normalized area value of the molecular water peak increased by ~80%, accompanied by the constant decrease in the area of HKUST-1 peaks (Figure 2c). According to the evolution of the spectral area presented in Figure 2d, the carboxylate group vibrations at 1646 and 1374 cm⁻¹ were primarily affected over ring deformation at 725 cm⁻¹, due to the stronger effect of water on the former. Since there are overlaps between the MOF and drug molecule vibrational modes within regions I and II (e.g., peaks at 759, 1374, 1450, and 1646 cm⁻¹), the decrease in the intensity of the most affected HKUST-1 peaks cannot be taken simply as the chemical decomposition of the host framework but might also be attributed to the progressive release of the drug molecules

from the HKUST-1 pores. Therefore, complementary measurements of HKUST-1/PU (Figure S11) and PU membranes (Figure S12) were performed to investigate any possible framework decomposition (discussed in detail below).

As recently reported by some of us,¹⁰ the encapsulation of the drug molecule via the mechanochemical in situ strategy results in the self-assembly of drug@MOF systems, in which (guest) drug molecules are successfully confined in the pores of the (host) HKUST-1 framework. We employed ab initio density functional theory (DFT) calculations using the periodic code CRYSTAL17²⁷ (see details in Methods) to reveal the nature of the guest–host interactions from different possible assemblies of 5-FU@HKUST-1 (i.e., adducts A–D in Figures S13–16). The calculations were performed with a newly developed DFT-based “composite method” PBEsol0-3c,²⁸ which uses a sol-def2-mSVP basis set (see details in Methods and Figure S17). On the basis of the electrostatic potential map of HKUST-1 and 5-FU (Figure S18a), it can be clearly seen that on the one hand, Cu atoms in the paddle-wheel of HKUST-1 (positive regions) can act as primary adsorption sites, while, on the other hand, oxygen atoms of 5-FU (negative regions) can strongly interact with copper through dative bonding. Instead, a less strong interaction is expected through the fluorine atom. In addition, the size of the 5-FU molecule and the Cu–Cu distances in the cage are commensurate to each other and can lead to a bridging conformation of the possible 5-FU@HKUST-1 adducts. We have then investigated the stabilization energy of four different drug–MOF binding configurations (i.e., adducts A–D in Figures S13–16) and contrasted it against the water–MOF interactions. The theoretical spectra for the adduct configurations being considered are presented in Figure 3a–d and were contrasted against the experimental 5-FU@HKUST-1 attenuated total reflectance (ATR)-FTIR spectrum.

The closer match between the experimental and theoretical spectrum of adduct A suggests that this is probably the dominant configuration in 5-FU@HKUST-1 system. Our theoretical results crucially show that 5-FU are in coordination with HKUST-1 specifically via its coordinatively unsaturated metal sites (CUS) (via $C=O \cdots Cu$ coordination). Concomitantly 5-FU establishing hydrogen bonds with the oxygen atoms present in the carboxylate groups, as depicted in Figure 3e. This configuration is akin to another reported system termed: TCNQ@HKUST-1.²⁹ However, on the basis of the computed binding energies summarized in Figure S18b and the analysis of the low energy vibrational bands (i.e., terahertz vibrations) via inelastic neutron scattering displayed in Figure S19, we found that a coexistence between the different adduct configurations is possible in the 5-FU@HKUST-1 system. According to the binding energies calculated, we established that D_2O and H_2O are capable of triggering the release of 5-FU, as observed experimentally (see Figure S18b and Table S4 for further details). Because of the smaller size of water molecules in comparison with 5-FU, the configurational entropy,³⁰ as well as entropy of stabilization,³¹ will favor the formation of water-CUS interactions in the HKUST-1 framework. A closer look at the redshift of the vibrational band at 1590 cm^{-1} displays two important findings. First, it indicates changes in the environment of the carboxylate group bridging the pores of the host framework. This could be a result of structural distortions to the framework unit cell,³² resulting in a low symmetry configuration (e.g., Cu–Cu distances in two adjacent paddlewheels; Figure 3f). Interestingly, we have established that the cubic structure of HKUST-1 is recoverable upon the release of the encapsulated drug as demonstrated by the powder X-ray diffraction (PXRD) patterns in Figure S20. Together, these interactions not only modify the environment of the paddlewheel structure of HKUST-1 but also affect the preferred spatial orientation, resulting in a mechanically strained framework. The recovery of the long-range framework periodicity suggests that the coordination of the carboxylate groups is also affected by guest encapsulation and is progressively restored during the release process, as seen in Figure 2a. Upon the departure of 5-FU, the main HKUST-1 bands become sharper, indicating the increase in the structure symmetry and the relaxation of the structure.^{33,34}

We want to emphasize that the permeation of water into the polymeric membrane was only possible because of the presence of HKUST-1 crystals embedded in these composites. We hypothesize that HKUST-1 enables the establishment of hydrophilic “channels” that facilitate the penetration of molecular water that triggers the release of the 5-FU drug molecules, as illustrated in Figure 4a. The role played by HKUST-1 on the water diffusion, attributed to the hydrophilic metal sites present in its structure, can be detected by contrasting the evolution of 5-FU/PU and 5-FU@HKUST-1/PU spectra (see Figure 2a and b). During measurements of 5-FU/PU membrane under static conditions, only minor changes to the drug peaks were observed in the FTIR spectra, in which a slower and smaller decrease in the spectral area (Figure 2b) was captured. In 5-FU@HKUST-1/PU spectra, we can observe reductions of as much as 90% in the intensity of drug molecule vibrational modes; however, in the 5-FU/PU spectra, the corresponding decline reaches a maximum of $\sim 35\%$. Further verification of the role of HKUST-1 on water accessibility can be observed in a demonstration presented in Figure S21. The change in color of HKUST-1/PU membrane upon heating

demonstrates that the water molecules, coordinated to the CUS, have accessibility into and out of the membrane. This effect has been further quantified by measuring the swelling of the composite due to water uptake (Figure S22) and the decline of surface contact angle ($\sim 95\text{--}80^\circ$, see Figure S23) due to the incorporation of hydrophilic HKUST-1 to the hydrophobic PU matrix.

As discussed above, the main vibrational peaks of HKUST-1 have not suffered major degradation during the static experiments. In the HKUST-1/PU spectra it is possible to observe the progressive increase in intensity of the molecular water peak (Figure S11b), confirming the permeation of water. We found a decrease in the spectral area of the symmetric and asymmetric vibrations of carboxylate groups at 1646 and 1450 cm^{-1} . The most important observation from the HKUST-1/PU spectra is that the redshift of the symmetric stretch of the carboxylate group, observed in 5-FU@HKUST-1/PU, was not detected in the spectra of HKUST-1/PU composite. This confirms that the band shift observed during the release of the drug molecule is not related to the deuteration of the carboxylate group³⁵ but caused by changes in the guest–host interactions. At this point, it is uncertain whether the amount of D_2O in contact with the sample was insufficient to cause detectable framework degradation, or, if the polymer is effectively protecting the HKUST-1 crystals (since the MOF is fairly stable when a small amount of water is adsorbed).²⁶ This question is addressed using the flow-cell studies described below.

Flow-Cell Measurements. SR-microFTIR in situ flow experiments using a liquid flow-cell were conducted to investigate the possible degradation of HKUST-1 and the protective role conferred by the PU matrix (Figure 4). For measurement in D_2O flow, the media were allowed to flow for approximately 25 min before starting data collection, thus allowing the system to reach D–H equilibrium. Over a total period of 2.3 h, no clear decomposition of the framework was observed. All the main framework peaks appear to be intact, with minimal changes to the carboxylate vibrations intensity (see in Figure 4b). Importantly, this confirms that the polymer matrix is able to significantly enhance the stability of HKUST-1 in aqueous conditions by providing a protective coating to the MOF structure. This can be further confirmed by contrasting the PXRD of HKUST-1/PU membrane and HKUST-1 powder before and after immersion in H_2O (Figure S24). While in the polymer composite the diffraction peaks of HKUST-1 appear to be intact, those in the powder sample suffers major degradation over a much shorter period of time.

Flow experiments were also conducted on 5-FU/PU membranes to further corroborate the difficulty that 5-FU molecules face to escape the PU membrane in the absence of HKUST-1 crystals. The evolution of the vibrational spectra is presented in Figure 4c showing the stabilization of the D_2O flow by the decrease in intensity of H–O–D bending mode ($\sim 1460\text{ cm}^{-1}$). A closer look at the drug peaks in the composite spectra reveals that their intensity is only minimally affected over a 2 h period (see Figure S25). This is more evident when 5-FU/PU spectra are contrasted against the spectra of 5-FU@HKUST-1/PU membrane (Figure 2a), in which changes to the drug peaks intensity were observed within 1 h (see Figure 2a). This observation highlights the importance of HKUST-1 embedded within the composites to yield a more sustained release of the drug. As previously discussed, the creation of the hydrophilic channels by HKUST-1 is essential for the water-CUS interactions and subsequent release of the drug molecule. Our

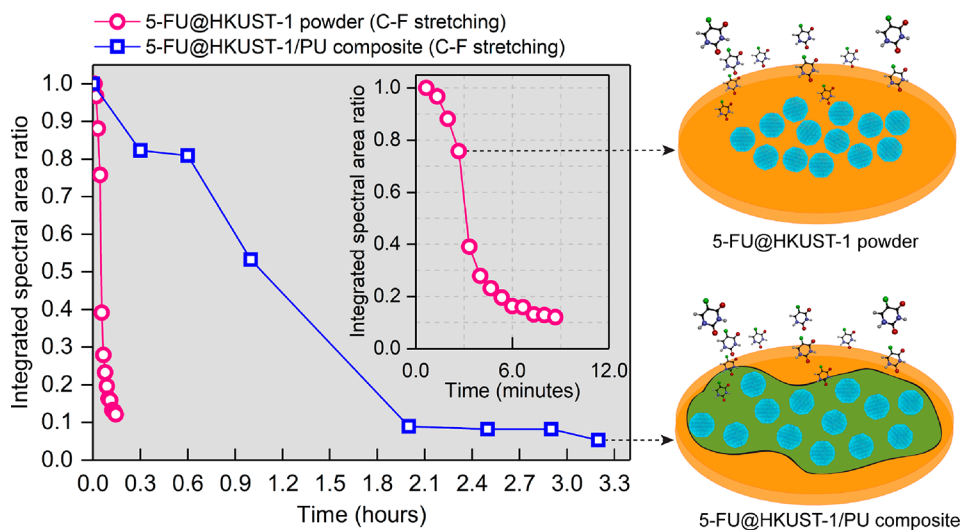


Figure 5. Changes in the rate of drug release due to the presence of the polymer matrix. Comparison of spectral area of 5-FU peak (C–F stretching- 1279 cm^{-1}) in 5-FU@HKUST-1 powder and 5-FU@HKUST-1/PU composite demonstrating how PU aids in regulating the velocity of 5-FU release.

results suggest that the polymer coating provides not only a supporting scaffold to the framework, protecting it against water degradation, but also helps to regulate the rate of the drug release process, as evidenced in Figure 5. In fact, the presence of the PU, even at a high HKUST-1:PU ratio, demonstrated the potential of employing the composites to suppress the release of 5-FU by a factor of about 20 times. Crucially, since HKUST-1 plays a key role on the release kinetics of 5-FU molecules (as demonstrated in Figures 2 and 4), one can conclude that the larger the HKUST-1:PU ratio, the faster the release of the guest molecules will be. Therefore, there is scope to tune the MOF:polymer ratio in the composites to achieve a well-controlled release of 5-FU molecules to mitigate the unwanted burst effect.

In this context, Figure 6 presents the spectra of 5-FU@HKUST-1 powder collected during flow experiments. The combination of measurements taken under D_2O (Figure 6a–c) and H_2O (Figure 6d) flow permitted a close monitoring of the evolution of 5-FU peaks in regions I and II of the vibrational spectra. Figure 6a presents the evolution of the sample over time under D_2O flow (the spectra of various time points were omitted for clarity). However, all the spectra collected have been represented for regions of interest within the spectral range in the 3D contour maps presented in Figure 6b and 6c and in the inset of Figure 6a. Under D_2O flow, the most pronounced changes can be observed in the shoulder at ~ 1620 and $\sim 1700\text{ cm}^{-1}$, which can be attributed to the C=C stretching of 5-FU. The progressive decline in the intensity of these peaks, accompanied by the sharpening of the HKUST-1 bands at 1374 , 1450 , and 1646 cm^{-1} , respectively, indicating the release of the 5-FU molecules. Meanwhile, it is possible to observe with detail the disappearance of these shoulders with time (Figure 6b and c). Figure 6d shows the spectra of 5-FU@HKUST-1 powder collected under H_2O flow. As can be seen in the highlighted region (1160 – 1300 cm^{-1}) and in the 2D profile presented in the inset, the release of the drug molecules upon exposure of HKUST-1 to a moist environment happens in an accelerated manner. By monitoring the evolution of the C–F stretching mode of 5-FU at 1279 cm^{-1} , indeed we detected the fast release of 5-FU molecules within only 10 min. This phenomenon marks the burst effect (rapid and uncontrolled release), which could be

attributed to the water-induced degradation of the HKUST-1 framework. The comparison of 5-FU@HKUST-1 powder spectra before and after exposure to a moist environment for over 9 h shows the pronounced decomposition of the powder sample with degradation of the main framework peaks as well as the disappearance of drug peaks (marked by asterisks in Figure S26). The increase in intensity of the band at 1720 cm^{-1} , associated with the C=O stretching of a carboxylic acid group, indicates the presence of protonated linker (i.e., H_3BTC). The protonation of the organic ligand is an indicator of major framework decomposition.^{36,37} Given this strong structural degradation, it becomes evident the need of the (hydrophobic) polymeric scaffolding for the protection of the (hydrophilic) HKUST-1 framework.

CONCLUSIONS

HKUST-1 plays a significant role in the basic and applied fields of MOFs research, not only due to its ease of synthesis and scalability but also because it is a reference material for the study of many general properties of MOFs. In this work, we have demonstrated that high-resolution synchrotron microspectroscopy is a powerful technique to track the local chemical and physical transformations taking place in the guest@MOF assembly and guest@MOF/Polymer composite during the dynamic release of guest molecules. We have discovered that while PU effectively and efficiently protects the moisture-sensitive MOF structure against water degradation, the incorporation of HKUST-1 is important to facilitate the release of the 5-FU the drug guest molecules. To this end, the combination of a hydrophilic MOF encapsulated drug with a hydrophobic polymeric matrix is a highly promising strategy to overcome the burst effect. Our DFT calculations uncover the preferred 5-FU@HKUST-1 configurations and elucidate the energetics behind the guest–host interactions. Furthermore, the theory sheds light on how the HKUST-1 recovers its symmetry upon the release of the encapsulated drug molecules, helping to confirm the efficacy of the solvent-free mechanochemical approach to manufacture drug@MOF assemblies employing a green chemical process. Finally, the general concept of tunable composite systems coupled with facile encapsulation of guests is

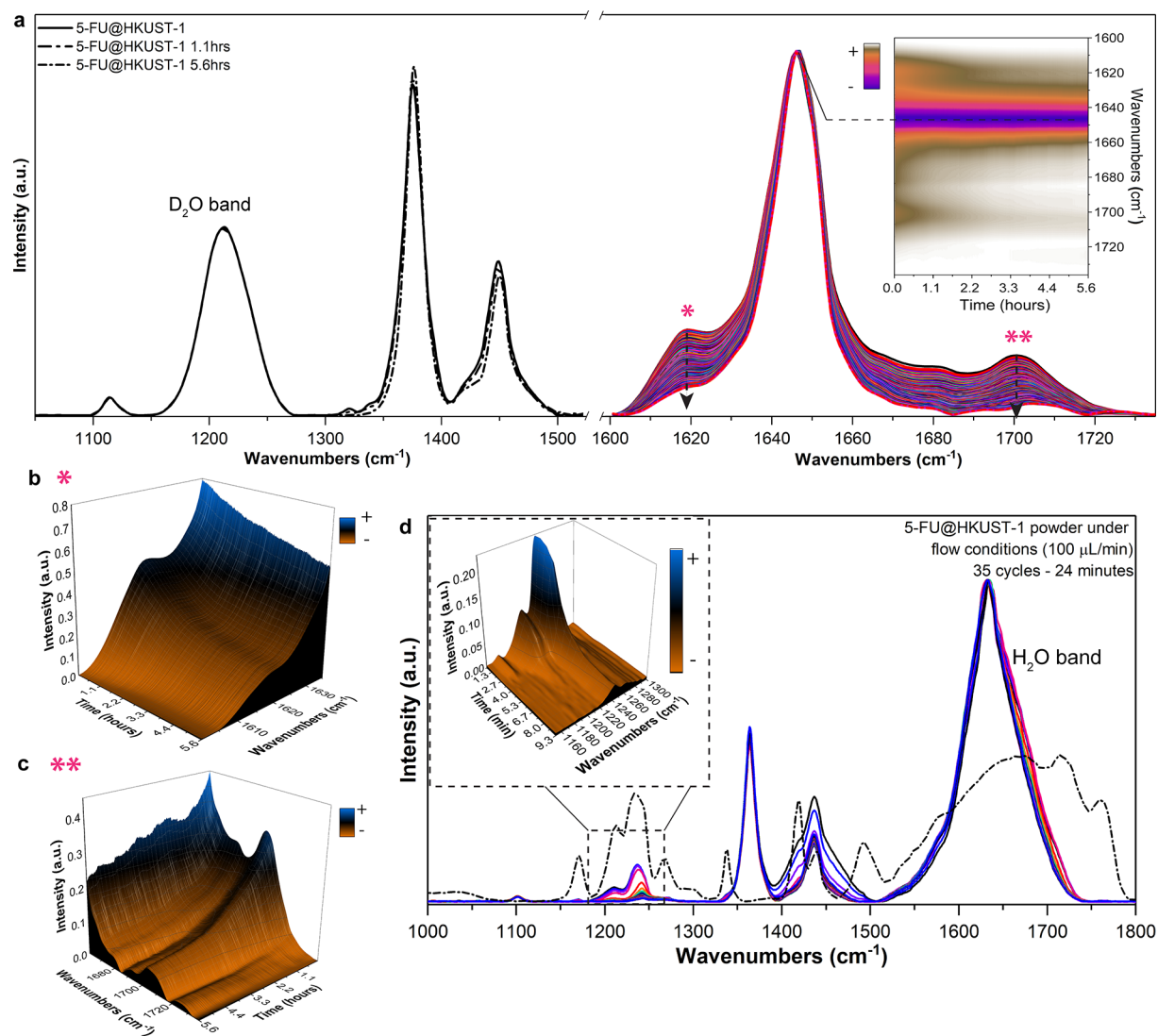


Figure 6. Flow-cell measurements of powder samples. (a) Time-resolved SR-microFTIR spectra of 5-FU@HKUST-1 powder sample collected under $100 \mu\text{L min}^{-1}$ of D_2O flow. The D_2O bending mode is indicated. Inset shows the 2D profile demonstrating the progressive decrease of the 5-FU drug peaks intensity. Asterisks mark the 5-FU peaks being monitored. (b, c) 3D contour maps showing the detailed evolution of the intensity of C=C bending and N-H stretching modes of the drug molecule. (d) Spectra of 5-FU@HKUST-1 powder sample collected under $100 \mu\text{L min}^{-1}$ H_2O flow. The H_2O bending mode is indicated. Inset displays the evolution of the C-F stretching mode ($\sim 1279 \text{ cm}^{-1}$) of 5-FU, indicating the fast release of a considerable amount of the drug molecule within 10 min. 5-FU spectrum was scaled down by a factor of 0.6 to facilitate the comparison with the spectra of the composite membranes molecules.

a promising way forward to controlling the binding and release of drug molecules confined in a range of microporous materials.

■ ASSOCIATED CONTENT

Supporting Information

The Supporting Information is available free of charge at <https://pubs.acs.org/doi/10.1021/acsami.9b21321>.

Full details of the synthetic procedures, DFT calculations, material characterization (TGA, SEM, AFM, and PXRD), and drug release studies (SR-microFTIR) (PDF)

■ AUTHOR INFORMATION

Corresponding Authors

Bartolomeo Civalleri – University of Turin, Torino, Italy;

orcid.org/0000-0003-3198-3161;

Email: bartolomeo.civalleri@unito.it

Jin-Chong Tan – University of Oxford, Oxford, U.K.;

orcid.org/0000-0002-5770-408X; Email: jin-chong.tan@eng.ox.ac.uk

Other Authors

Barbara E. Souza – University of Oxford, Oxford, U.K.

Lorenzo Donà – University of Turin, Torino, Italy

Kirill Titov – University of Oxford, Oxford, U.K.

Paolo Bruzzese – University of Turin, Torino, Italy

Zhixin Zeng – University of Oxford, Oxford, U.K.

Yang Zhang – University of Oxford, Oxford, U.K.

Arun S. Babal – University of Oxford, Oxford, U.K.

Annika F. Möslein – University of Oxford, Oxford, U.K.

Mark D. Frogley – Diamond Light Source, Chilton, United Kingdom

Magda Wolna – Diamond Light Source, Chilton, United Kingdom

Gianfelice Cinque – Diamond Light Source, Chilton, United Kingdom

Complete contact information is available at:
<https://pubs.acs.org/10.1021/acsami.9b21321>

Notes

The authors declare no competing financial interest.

ACKNOWLEDGMENTS

B.E.S. thanks the Minas Gerais Research Foundation (FAPEMIG CNPJ n21.949.888/0001-83) for a DPhil scholarship award. J.C.T. thanks the EPSRC Grant EP/N014960/1 and ERC Consolidator Grant under the grant agreement 771575 (PROMOFS) for funding. We acknowledge the Diamond Light Source for the award of beamtime no. SM14902 and SM20281 at beamline B22 MIRIAM. We are grateful to the Research Complex at Harwell (RCAH) for the provision of advanced materials characterization facilities.

REFERENCES

- (1) Márquez, A. G.; Hidalgo, T.; Lana, H.; Cunha, D.; Blanco-Prieto, M. J.; Alvarez-Lorenzo, C.; Boissière, C.; Sánchez, C.; Serre, C.; Horcajada, P. Biocompatible Polymer-Metal-Organic Framework Composite Patches for Cutaneous Administration of Cosmetic Molecules. *J. Mater. Chem. B* **2016**, *4*, 7031–7040.
- (2) Li, H.; Lv, N.; Li, X.; Liu, B.; Feng, J.; Ren, X.; Guo, T.; Chen, D.; Fraser Stoddart, J.; Gref, R.; Zhang, J. Composite CD-MOF Nanocrystals-Containing Microspheres for Sustained Drug Delivery. *Nanoscale* **2017**, *9*, 7454–7463.
- (3) Deng, K.; Hou, Z.; Li, X.; Li, C.; Zhang, Y.; Deng, X.; Cheng, Z.; Lin, J. Aptamer-Mediated Up-Conversion Core/Mof Shell Nanocomposites for Targeted Drug Delivery and Cell Imaging. *Sci. Rep.* **2015**, *5*, 7851.
- (4) Orellana-Tavra, C.; Baxter, E. F.; Tian, T.; Bennett, T. D.; Slater, N. K. H.; Cheetham, A. K.; Fairen-Jimenez, D. Amorphous Metal-Organic Frameworks for Drug Delivery. *Chem. Commun.* **2015**, *51*, 13878–13881.
- (5) Horcajada, P.; Serre, C.; Maurin, G.; Ramsahye, N. A.; Balas, F.; Vallet-Regi, M.; Sebban, M.; Taulelle, F.; Ferey, G. Flexible Porous Metal-Organic Frameworks for a Controlled Drug Delivery. *J. Am. Chem. Soc.* **2008**, *130*, 6774–6780.
- (6) Senapati, S.; Mahanta, A. K.; Kumar, S.; Maiti, P. Controlled Drug Delivery Vehicles for Cancer Treatment and Their Performance. *Signal Transduct. Target. Ther.* **2018**, *3*, 7.
- (7) Ferrari, R.; Sponchioni, M.; Morbidelli, M.; Moscatelli, D. Polymer Nanoparticles for the Intravenous Delivery of Anticancer Drugs: The Checkpoints on the Road from the Synthesis to Clinical Translation. *Nanoscale* **2018**, *10*, 22701–22719.
- (8) Fan, W.; Lu, N.; Shen, Z.; Tang, W.; Shen, B.; Cui, Z.; Shan, L.; Yang, Z.; Wang, Z.; Jacobson, O.; Zhou, Z.; Liu, Y.; Hu, P.; Yang, W.; Song, J.; Zhang, Y.; Zhang, L.; Khashab, N. M.; Aronova, M. A.; Lu, G.; Chen, X. Generic Synthesis of Small-Sized Hollow Mesoporous Organosilica Nanoparticles for Oxygen-Independent X-Ray-Activated Synergistic Therapy. *Nat. Commun.* **2019**, *10*, 1241.
- (9) Huang, X.; Brazel, C. S. On the Importance and Mechanisms of Burst Release in Matrix-Controlled Drug Delivery Systems. *J. Controlled Release* **2001**, *73*, 121–136.
- (10) Souza, B. E.; Rudic, S.; Titov, K.; Babal, A. S.; Taylor, J. D.; Tan, J. C. Guest-Host Interactions of Nanoconfined Anti-Cancer Drug in Metal-Organic Framework Exposed by Terahertz Dynamics. *Chem. Commun.* **2019**, *55*, 3868–3871.
- (11) Todaro, M.; Buscarino, G.; Sciortino, L.; Alessi, A.; Messina, F.; Taddei, M.; Ranocchiaro, M.; Cannas, M.; Gelardi, F. M. Decomposition Process of Carboxylate MOF HKUST-1 Unveiled at the Atomic Scale Level. *J. Phys. Chem. C* **2016**, *120*, 12879–12889.
- (12) Domán, A.; Czakkel, O.; Porcar, L.; Madarász, J.; Geissler, E.; László, K. Role of Water Molecules in the Decomposition of HKUST-1: Evidence from Adsorption, Thermoanalytical, X-Ray and Neutron Scattering Measurements. *Appl. Surf. Sci.* **2019**, *480*, 138–147.
- (13) Zhang, F.; Hu, C.; Kong, Q.; Luo, R.; Wang, Y. Peptide-/Drug-Directed Self-Assembly of Hybrid Polyurethane Hydrogels for Wound Healing. *ACS Appl. Mater. Interfaces* **2019**, *11*, 37147–37155.
- (14) Wang, W.; Wang, C. Polyurethane for Biomedical Applications: A Review of Recent Developments. In *The Design and Manufacture of Medical Devices*; Woodhead Publishing Reviews: Mechanical Engineering Series; Woodhead Publishing, 2012; pp 115–151.
- (15) Chen, X.; Liu, W.; Zhao, Y.; Jiang, L.; Xu, H.; Yang, X. Preparation and Characterization of Peg-Modified Polyurethane Pressure-Sensitive Adhesives for Transdermal Drug Delivery. *Drug Dev. Ind. Pharm.* **2009**, *35*, 704–711.
- (16) Shih, Y. H.; Kuo, Y. C.; Lirio, S.; Wang, K. Y.; Lin, C. H.; Huang, H. Y. A Simple Approach to Enhance the Water Stability of a Metal-Organic Framework. *Chem. - Eur. J.* **2017**, *23*, 42–46.
- (17) Ren, X.; Yang, C.; Zhang, L.; Li, S.; Shi, S.; Zhang, X.; Wang, R.; Sun, J.; Yue, T.; Wang, J. Copper Metal-Organic Framework Loaded on Chitosan Film for Efficient Inhibition of Bacteria and Therapy of Local Infection. *Nanoscale* **2019**, *11*, 11830–11838.
- (18) Xiao, J.; Zhu, Y.; Huddleston, S.; Li, P.; Xiao, B.; Farha, O. K.; Ameer, G. A. Copper Metal-Organic Framework Nanoparticles Stabilized with Folic Acid Improve Wound Healing in Diabetes. *ACS Nano* **2018**, *12*, 1023–1032.
- (19) D'Souza, S. A Review of in Vitro Drug Release Test Methods for Nano-Sized Dosage Forms. *Adv. Pharm.* **2014**, *2014*, 304757.
- (20) Roth Stefaniak, K.; Epley, C. C.; Novak, J. J.; McAndrew, M. L.; Cornell, H. D.; Zhu, J.; McDaniel, D. K.; Davis, J. L.; Allen, I. C.; Morris, A. J.; Grove, T. Z. Photo-Triggered Release of 5-Fluorouracil from a MOF Drug Delivery Vehicle. *Chem. Commun.* **2018**, *54*, 7617–7620.
- (21) Rojas, S.; Guillou, N.; Horcajada, P. Ti-Based NanoMOF as an Efficient Oral Therapeutic Agent. *ACS Appl. Mater. Interfaces* **2019**, *11*, 22188–22193.
- (22) Rojas, S.; Baati, T.; Njim, L.; Manchego, L.; Neffati, F.; Abdeljelil, N.; Saguem, S.; Serre, C.; Najjar, M. F.; Zakhama, A.; Horcajada, P. Metal-Organic Frameworks as Efficient Oral Detoxifying Agents. *J. Am. Chem. Soc.* **2018**, *140*, 9581–9586.
- (23) Doherty, J.; Raoof, A.; Hussain, A.; Wolna, M.; Cinque, G.; Brown, M.; Gardner, P.; Denbigh, J. Live Single Cell Analysis Using Synchrotron FTIR Microspectroscopy: Development of a Simple Dynamic Flow System for Prolonged Sample Viability. *Analyst* **2019**, *144*, 997–1007.
- (24) Elsheikha, H. M.; Elsaied, N. A.; Chan, K. L. A.; Brignell, C.; Harun, M. S. R.; Wehbe, K.; Cinque, G. Label-Free Characterization of Biochemical Changes within Human Cells under Parasite Attack Using Synchrotron Based Micro-FTIR. *Anal. Methods* **2019**, *11*, 2518–2530.
- (25) Dhupal, N. R.; Singh, M. P.; Anderson, J. A.; Kiefer, J.; Kim, H. J. Molecular Interactions of a Cu-Based Metal-Organic Framework with a Confined Imidazolium-Based Ionic Liquid: A Combined Density Functional Theory and Experimental Vibrational Spectroscopy Study. *J. Phys. Chem. C* **2016**, *120*, 3295–3304.
- (26) Mason, J. A.; Veenstra, M.; Long, J. R. Evaluating Metal-Organic Frameworks for Natural Gas Storage. *Chem. Sci.* **2014**, *5*, 32–51.
- (27) Dovesi, R.; Erba, A.; Orlando, R.; Zicovich-Wilson, C. M.; Civalieri, B.; Maschio, L.; Rérat, M.; Casassa, S.; Baima, J.; Salustro, S.; Kirtman, B. Quantum-Mechanical Condensed Matter Simulations with Crystal. *Wiley Interdiscip. Rev. Comput. Mol. Sci.* **2018**, *8*, e1360.
- (28) Dona, L.; Brandenburg, J. G.; Civalieri, B. Extending and Assessing Composite Electronic Structure Methods to the Solid State. *J. Chem. Phys.* **2019**, *151*, 121101.
- (29) Talin, A. A.; Centrone, A.; Ford, A. C.; Foster, M. E.; Stavila, V.; Haney, P.; Kinney, R. A.; Szalai, V.; El Gabaly, F.; Yoon, H. P.; Leonard, F.; Allendorf, M. D. Tunable Electrical Conductivity in Metal-Organic Framework Thin-Film Devices. *Science* **2014**, *343*, 66–69.

(30) Fleck, M.; Zagrovic, B. Configurational Entropy Components and Their Contribution to Biomolecular Complex Formation. *J. Chem. Theory Comput.* **2019**, *15*, 3844–3853.

(31) Rost, C. M.; Sachet, E.; Borman, T.; Moballeggh, A.; Dickey, E. C.; Hou, D.; Jones, J. L.; Curtarolo, S.; Maria, J. P. Entropy-Stabilized Oxides. *Nat. Commun.* **2015**, *6*, 8485.

(32) Sutton, C. C.; da Silva, G.; Franks, G. V. Modeling the Ir Spectra of Aqueous Metal Carboxylate Complexes: Correlation between Bonding Geometry and Stretching Mode Wavenumber Shifts. *Chem.-Eur. J.* **2015**, *21*, 6801–6805.

(33) Petit, C. *Factors Affecting the Removal of Ammonia from Air on Carbonaceous Materials: Investigation of Reactive Adsorption Mechanism*; Springer Science & Business Media: New York, USA, 2012.

(34) Seo, Y. K.; Hundal, G.; Jang, I. T.; Hwang, Y. K.; Jun, C. H.; Chang, J. S. Microwave Synthesis of Hybrid Inorganic-Organic Materials Including Porous $\text{Cu}_3(\text{BTC})_2$ from Cu(II)-Trimesate Mixture. *Microporous Mesoporous Mater.* **2009**, *119*, 331–337.

(35) Resler, T.; Schultz, B. J.; Lorenz-Fonfria, V. A.; Schlesinger, R.; Heberle, J. Kinetic and Vibrational Isotope Effects of Proton Transfer Reactions in Channelrhodopsin-2. *Biophys. J.* **2015**, *109*, 287–297.

(36) Mahmoodi, N. M.; Abdi, J.; Oveisi, M.; Alinia Asli, M.; Vossoughi, M. Metal-Organic Framework (Mil-100 (Fe)): Synthesis, Detailed Photocatalytic Dye Degradation Ability in Colored Textile Wastewater and Recycling. *Mater. Res. Bull.* **2018**, *100*, 357–366.

(37) Lin, S.; Song, Z.; Che, G.; Ren, A.; Li, P.; Liu, C.; Zhang, J. Adsorption Behavior of Metal-Organic Frameworks for Methylene Blue from Aqueous Solution. *Microporous Mesoporous Mater.* **2014**, *193*, 27–34.